

## A PLANAR 4.0 GHz REACTIVELY STEERED ADAPTIVE ARRAY

Robert J. Dinger

Naval Weapons Center, China Lake, CA 93555

## ABSTRACT

A planar reactively steered adaptive array comprised of a single active microstrip element and eight closely coupled parasitic microstrip elements is described. Null steering is accomplished by adaptive control of reactive terminations on the parasitic elements using both a steepest descent algorithm and a guided random search algorithm. The planar array can steer nulls in elevation and azimuth with a depth of about 35 dB.

## INTRODUCTION

Adaptive arrays reduce the energy of an incident interference signal reaching a receiver by steering an antenna pattern null in the direction of the interference. The typical adaptive array employs a controllable complex weight on each array element, and the weighted element outputs are combined in an electronic summing element to obtain the array output. Even though the term "adaptive" implies some accommodation to imperfections in the array environment, it has been found (1) that element spacings of  $0.25\lambda$  ( $\lambda$  = wavelength) or less degrade seriously the depth of a null that an adaptive array can form towards an interferer, due to the mutual coupling between the elements. This paper presents results for a planar array, known as a reactively steered adaptive array (RESAA), that can maintain deep nulls towards an interferer even when the element spacing is as small as  $0.1\lambda$ .

A RESAA, shown in Fig. 1, has only a single element that is connected by a transmission line to a receiver. The remaining elements are parasitic, and the pattern is formed according to the values of the reactive terminations on these parasitic elements. The basic scheme of a reactively steered array was first proposed by Harrington (2) for deterministic control; over the last several years, we have been applying this idea to adaptive arrays (3-5) using a linear array of microstrip patch elements resonant at 4.0 GHz. Using steepest descent adaptive control with serial adjustment of the loads, the microstrip array has demonstrated an ability to steer a null

in the plane of the elements with a depth of over 30 dB and width of about 25 deg.

The earlier work employed linear arrays with a relatively small number of elements (usually five). Herein, we present recent results on a planar array of nine elements arranged in a cross configuration. The extension of the linear array results to planar arrays is not a trivial problem. The doubling of the number of controlled loads (from four to eight) presents problems in convergence speed for a control algorithm using serial adjustment of the loads; hence, parallel algorithms--inherently more complicated--are required.

## EXPERIMENTAL CONFIGURATION

Figure 2 shows the five by five cross configuration of the array. Each element is  $1.0 \times 2.33$  cm on a 1.58-mm-thick Rexolite 1422 substrate and has a resonant frequency of 4.0 GHz. The center element of the cross is connected to the receiver; the reactive loads for the remaining elements are visible in Fig. 2.

The reactive loads are varactor-diode reflection phase shifters fabricated using standard microstrip circuit techniques. Approximately 250 deg of phase shift can be obtained with a bias voltage range of 0 to -10 V.

In Fig. 3 we show the array configured for closed-loop operation on a rooftop test range. The array was operated in a power inversion mode (6) with no reference or "desired" signal, so that the algorithm acted to reduce the power appearing at the receiver from any and all signals incident on the array. Since the power meter used as a receiver in these measurements had a relatively long integration time (one-half second), actual elapsed times were meaningless, so that convergence times below are given in terms of number of iterations.

## CONTROL ALGORITHMS

We have investigated two control algorithms for the planar array. The first is a steepest descent algorithm (6) that is a straightforward extrapolation of the version used for the five-element linear array. Denoting  $X$  as a vector

whose components are the reactive loads, the value of  $\mathbf{X}$  at the  $(j+1)$ th step is related to the value at the  $j$ th step by

$$\mathbf{x}(j+1) = \mathbf{x}(j) - KV \quad , \quad (1)$$

where  $K$  is a positive constant that controls the convergence rate and  $V$  is the receiver output. In order to determine each component of the gradient operator in Eq. (1), each reactive load is dithered sequentially by an amplitude  $\Delta X$  and the received power measured, so that a single iteration requires  $(N-1)$  measurements of the receiver output. Since the receiver power measurement and subsequent analog-to-digital conversion are relatively time-consuming, a faster algorithm is needed that requires only a single power measurement for each iteration.

Guided random search (7) is such an algorithm. In guided random search, the new value of  $\mathbf{X}$  is chosen according to

$$\mathbf{x}(j+1) = \mathbf{x}(j) + \mathbf{x}(j) \quad , \quad (2)$$

where  $\mathbf{x}(j)$  is a vector whose components are selected from  $(N-1)$  Gaussian sequences with zero mean and variance  $\sigma$ . At each iteration, the components of  $\mathbf{x}$  are derived from a random number generator, the new values of  $\mathbf{X}$  are entered simultaneously, and then only a single reading of the receiver is made. If this choice of  $\mathbf{x}(j)$  reduces the interference power, the new value of  $\mathbf{X}$  is used as the starting point for the next iteration; otherwise, a new trial  $\mathbf{x}(j)$  is selected.

#### EXPERIMENTAL RESULTS

Figures 4 through 6 are the results of one run taken for an interference source incident from an angle of  $-45$  deg in azimuth and  $+25$  deg in elevation. Figure 4 shows the received interference power at each iteration, displaying the reduction in interference power as the array adapts. Not included in Fig. 4 are 10 initial random search steps, the purpose of which is to find an initial point for the steepest descent processing that is in the neighborhood of the optimum point. Since the interference power is  $-24$  dBm before adaptation, the initial random search lowers the interference power by  $14$  dB and steepest descent processing lowers it by an additional  $22$  dB.

Figure 5 is a contour plot of the null in a portion of the transverse plane. A significant point of this figure is that the null is well confined in both the azimuth and elevation directions, with a response  $18$  dB above the null depth at angles  $15$  deg from the desired null direction. Figure 6 shows antenna patterns taken at two cuts. Figure 7 is another example of a contour plot taken for a null formed on a signal incident at antenna boresight.

The examples shown in Figs. 4 through 7 use the steepest descent method, but similar antenna patterns and interference reduction curves are

obtained with the guided random search method. The latter technique typically takes about five times the number of iterations for convergence, where a single iteration for each method is defined as a unit increase in  $j$  in Eq. (1) or (2). However, in view of the much fewer power readings needed per iteration for the guided random search method (one, vs eight for steepest descents), guided random search is about  $40\%$  faster than the steepest descent method. A value of  $\sigma = 0.15$  V (expressed in terms of the varactor-bias voltage) was found to be optimum for the guided random search method; this compares well with the value of  $\Delta X = 0.1$  V that was optimum for the steepest descent method. The nulling bandwidth, measured as described in (3), is approximately  $20$  MHz.

#### CONCLUSIONS

The RESAA technique has been extended from a linear array to a planar array and has demonstrated an ability to steer nulls in azimuth and elevation. The guided random search method offers a means of rapid control of a large number of reactively loaded parasitic elements.

The advantages of a RESAA, as compared with a conventional adaptive array, are twofold. The mixers and summing element usually needed for complex weighting and summing are eliminated; better control of the pattern is achieved for compact arrays, since the mutual coupling is explicitly taken into account.

#### REFERENCES

- (1) I. J. Gupta and A. A. Ksienki, "Effect of Mutual Coupling on the Performance of Adaptive Arrays," IEEE Trans. Antennas Propag., Vol. AP-31, pp. 785-791, Sept. 1983.
- (2) R. F. Harrington, "Reactively Controlled Directive Arrays," IEEE Trans. Antennas Propag., Vol. AP-26, pp. 390-397, May 1978.
- (3) R. J. Dinger, "Reactively Steered Adaptive Array Using Microstrip Patch Elements at 4 GHz," IEEE Trans. Antennas Propag. (to be published).
- (4) R. J. Dinger, "A Microstrip Power Inversion Array Using Parasitic Elements," 1983 AP-S International Symposium Digest, Houston, TX, pp. 191-194, May 23-26, 1983.
- (5) R. J. Dinger, "Closed-Loop Adaptive Control of a 4.0 GHz Reactively Steered Microstrip Array: Experimental Results," Naval Weapons Center Report TP 6481, Oct. 1983.
- (6) R. A. Monzingo and T. W. Miller, Introduction to Adaptive Arrays, New York: Wiley, 1980.
- (7) G. A. Bekey and W. J. Karplus, Hybrid Computation, New York: Wiley, 1969.

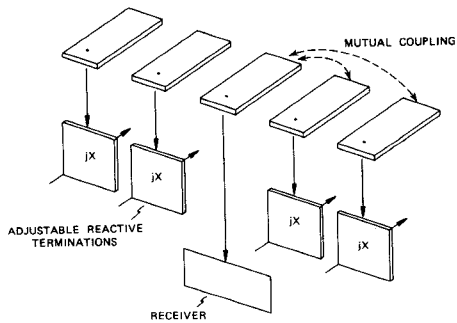


Fig. 1. Diagram of Reactively Steered Array.

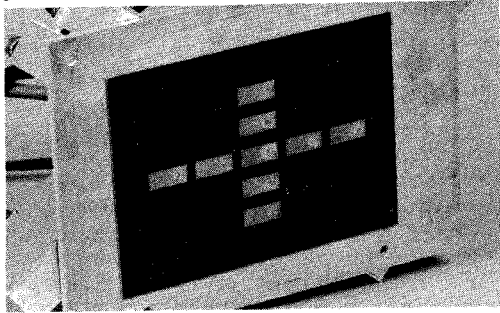


Fig. 2. Planar RESAA.

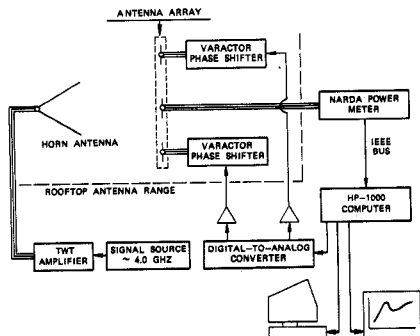


Fig. 3. Diagram of Test Setup.

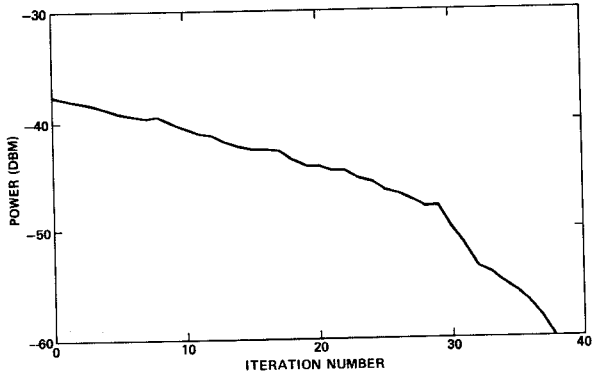


Fig. 4. Reduction in Interference Power During Steepest Descent Processing. The first 10 random search steps are not shown. Incident power before adaptation was -24 dBm.  $\Delta X = 0.1$  V,  $K = 0.01$ .

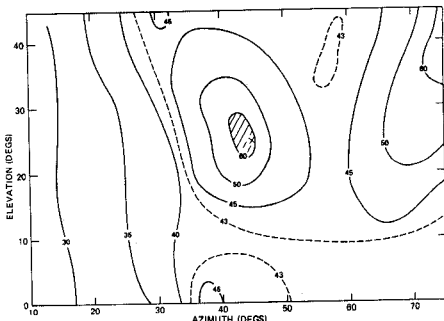


Fig. 5. Pattern Contour Plot for Adapted Pattern. Contours are in dBm (minus sign has been dropped for clarity). The cross indicates direction of interference during null formation.

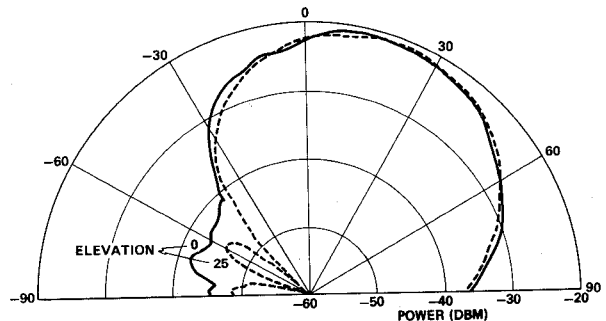


Fig. 6. Antenna Patterns. The azimuth angle is the polar variable, with patterns for two different elevations given. A value of -20 dBm corresponds to 7.0 dBi. The pattern is shown reversed in azimuth angle, so that (for example) -45 deg on this plot corresponds to +45 deg on Fig. 5.

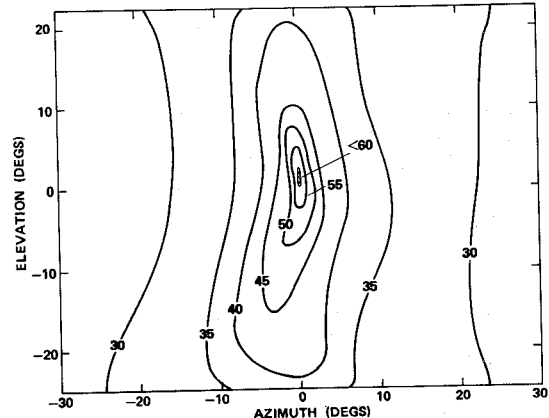


Fig. 7. Pattern Contour Plot for Interference Incident at Elev = 0 deg and Azimuth = 0 deg.